Kinetics and Modeling of Hybrid Core−Shell Nanoparticles Synthesized by Seeded Emulsion (Co)polymerization of Styrene and γ-Methacryloyloxypropyltrimethoxysilane

K. F. Ni,[†,‡,§] N. Sheibat-Othman,[*,§] G. R. Shan,[‡] G. Fevotte,[§] and E. Bourgeat-Lami[†]

Laboratoire de Chimie et Procédés de Polymérisation, UMR 140-CPE-BP2077-43, Bd. du 11 Nov. 1918-69616 Villeurbanne, France; State Key Laboratory of Polymerization Reaction Engineering, Department of Chemical Engineering, Zhejiang University, Hangzhou 310027, China; and Laboratoire d'Automatique et de Génie des Procédés, UMR 5007-Université Lyon1-CNRS/ESCPE, Bât 308, 43, Bd. du 11 Nov. 1918-69622 Villeurbanne, France

Received May 13, 2005; Revised Manuscript Received July 19, 2005

ABSTRACT: Core−shell nanoparticles with a polystyrene core and a hybrid copolymer shell are synthesized via emulsion polymerization of styrene and subsequent addition of γ-methacryloyloxypropyltrimethoxysilane (MPS) to produce the shell by copolymerization reaction of MPS with the residual amount of styrene. The kinetics of copolymerization and hydrolysis−condensation reaction are studied by gas chromatography (GC) and solid-state ^{29}Si NMR along with the emulsion polymerization process. A complete model of the reaction mechanisms is developed, and the results are compared with the experimental data.

Introduction

In recent years, organic−inorganic hybrid nanomaterials have attracted much interest because of their extensive potential application in various fields of material science, ranging from paints, magnetic fluids, and high-quality paper coating to catalysis, microelectronics, and biotechnology. Heterogeneous polymerization, especially emulsion polymerization, provides an effective way of synthesizing nanoparticles with various architectures and forms. The elaboration of hybrid materials by the combination of organic polymerization and inorganic polycondensation of vinyl monomers carrying functional groups reactive in the sol−gel process is of growing interest in recent literature.[1−7] However, this kind of elaboration is seldom applied in heterogeneous polymerization due to the simultaneous hydrolysis and condensation reaction of the metal alkoxide groups of the organosilane monomer during the polymerization process. The hydrolysis reaction is described by the following formula (more details are given in the modeling section):

$$-\mathrm{Si{-}OCH_3} + \mathrm{H_2O} \xrightarrow{k_\mathrm{h}} -\mathrm{Si{-}OH} + \mathrm{CH_3{-}OH} \quad \text{(a)}$$

and the condensation reaction is given by

$$-\mathrm{Si{-}OH} + -\mathrm{Si{-}OH} \xrightarrow{k_\mathrm{c}} -\mathrm{Si{-}O{-}Si}- + \mathrm{H_2O} \quad \text{(b)}$$

The simultaneous hydrolysis and condensation reactions make both the microstructure and morphology of the particles difficult to control. Few works focused on this field in polymeric systems[8] and in miniemulsion polymerization techniques,[6,7] and some works proposed pH control methods.[9] Most attention was paid to practical applications of the particles rather than to the analysis of the kinetics of the reaction.[10,11]

In a recent work, Tissot and Bourgeat-Lami[12−14] synthesized hybrid polymer latexes by emulsion polymerization using γ-methacryloyloxypropyltrimethoxysilane (MPS) as functional (co)monomer. The authors studied the influence of pH, concentration of MPS, and the surfactant nature on the latex particles size, morphology, and surface properties. In a recent work,[15] the authors studied the influence of the operating conditions on the copolymer microstructure and particles morphology during the preparation of core−shell nanoparticles with a polystyrene core and a hybrid copolymer shell. Kinetics and modeling of this process were not addressed in these works. Studying the kinetics and modeling of this system represents a real challenge because of the complexity of the reaction scheme. Indeed, two kinds of reactions (hydrolysis and condensation) take place simultaneously with the emulsion polymerization. These reactions influence the partitioning of monomer and therefore the polymerization rate.

Modeling of emulsion (co)polymerization has been extensively studied for decades of years. A recent review was proposed by Gao and Penlidis,[16] which summarizes various emulsion polymerization models from the classical theory to the latest advance in the modeling. Research on the kinetics and modeling of the sol−gel reaction of alkoxysilane molecules in homogeneous phase has also been carried out intensively. The main works are reviewed by Sefcik and McCormic[17] and Osterholtz and Pohl.[18] They presented the mechanisms, kinetics, and models of the hydrolysis−condensation reactions. At our knowledge, these models have never been applied in heterogeneous medium such as an emulsion polymerization medium.

In this work, modeling of emulsion polymerization is realized in the presence of a sol−gel process. Polymerization kinetics and transfer between the different phases are related to the rates of hydrolysis and condensation in the aqueous phase. The kinetics of hydrolysis and condensation reactions are studied by following the reactions using gas chromatography (GC) and ^{29}Si NMR. The modeling results are compared to

---

[†] UMR 140-CPE-BP2077-43.
[‡] Zhejiang University.
[§] UMR 5007-Université Lyon1-CNRS/ESCPE.

10.1021/ma050999g CCC: $30.25

Table 1. Monomer Concentrations in Water and Latex Particles under Saturation and the Partitioning Coefficients between the Different Phases (Measured Data)

	STY	MPS
monomer concn in latex particles (mol/cm^3)	5.5×10^{-3}	3.7×10^{-4}
monomer concn in water (mol/cm^3)	3.65×10^{-6}	1.4×10^{-5}
k_i^{p}	1507	25.8
k_i^{d}	2.37×10^3	364

the experimental data.

Experimental Section

Materials. Styrene (Aldrich) was distilled under vacuum before use. Potassium persulfate (KPS, Acros Organics) was used as initiator, and dodecyl thiol ($C_{12}H_{25}$−SH, Aldrich) was used as chain transfer agent. The surfactant used was *N*,*N*-dodecyldimethylammoniopropansulfonate (Ralufon, Aldrich) which was found in a previous work[9] to be an efficient stabilizer. Ammonium dihydrogen phosphate (99%, Acros), disodium hydrogen phosphate (99%, Prolabo), and sodium hydrogen carbonate (99.5%, Prolabo) were used as received. γ-Methacryloyloxypropyltrimethoxysilane (MPS, Aldrich) was used as supplied. The water was deionized on mixed bed resins.

Preparation of the Hybrid Core−Shell Nanoparticles. The hybrid core−shell nanoparticles were prepared in two steps. Emulsion homopolymerization of styrene was first carried out at 70 °C up to ~90% conversion, using KPS as initiator, dodecyl thiol as transfer agent, and Ralufon as surfactant. Then, a given amount of MPS was added to the suspension medium, and the copolymerization of styrene and MPS was continued until the final conversion was reached. The pH value of the suspension was fixed at 7 by adding equivalent quantities of ammonium dihydrogen phosphate and disodium hydrogen phosphate or at 8.5 by adding sodium hydrogen carbonate. A typical recipe was as follows: styrene, 60 g; KPS, 0.5 g; chain transfer agent, 2.4 g; surfactant, 0.8 g; buffer, 0.25 g; water, 240 g; and MPS, 6 or 18 g.

Measurement of the Monomer Saturation Concentration. After synthesis of the polystyrene seed while fixing the pH value at 7, some inhibitor was added to the suspension medium together with an excess of monomer. The system was then allowed to reach equilibrium under shaking at the required temperature. The phases (swollen polymer particles, monomer droplet, and aqueous phase) were separated by centrifuging at 21 000 rpm. The monomer concentration in the polymer particles was determined by GC after dissolving the swollen polymer particles in THF. The concentration of monomer in the aqueous phase was determined using THF as internal standard. The results for MPS and styrene are shown in Table 1.

Residual Concentrations. The overall and the individual monomer conversions and the rate of MPS hydrolysis (concentration of methanol) were measured by GC. Samples of latex are withdrawn as a function of time and dissolved in appropriate amounts of THF which was used as an internal standard for GC calibration. The hydrolysis reaction of MPS was also followed by GC from the ratios of the peak areas of methanol to THF.

The condensation reactions were followed by ^{29}Si solid-state NMR measurements. The samples were immediately cooled, centrifuged, and dried under vacuum. ^{29}Si solid-state NMR measurements were performed on a Bruker DSX-300 spectrometer operating at 59.6 MHz using cross-polarization of protons. The contact time was 5 ms, the recycle delay 1 s (sufficient for a full relaxation of protons), and the spinning rate 5 kHz. The ^{29}Si NMR spectra were simulated using the DM-FIT program for quantitative analysis.

Measurement of Kinetic Parameters. The hydrolysis and condensation rate coefficients were determined in ethanol−water solution by performing a series of ^{29}Si liquid-state NMR measurements after introducing 2.5 g of MPS into 5 g of solution buffered by adding equivalent quantities of ammonium dihydrogen phosphate and disodium hydrogen phosphate (pH = 7) or sodium hydrogen carbonate (pH = 8.5) at 70 °C. Identification can then be done based on these measurements by writing the material balance equations of hydrolysis and condensation[19,20] (see Table 2).

Table 2. Hydrolysis and Condensation Rate Coefficients at Different pH Values (Measured Data)

	k_{h} (s^{-1})	k_{c} (cm^3/(mol s))
pH = 7	3.83×10^{-4}	100
pH = 8.5	1.02×10^{-2}	

The condensation rate coefficient at pH = 8.5 cannot be accurately determined because the condensation is very fast. Actually, the silanol groups (SiOH) condense as soon as they are produced by hydrolysis. The condensation rate coefficient is therefore very important. The condensation reaction is in this case controlled by the hydrolysis rate.

Reaction Scheme. In this process, polystyrene cores are formed first by homopolymerization of styrene to around 90% conversion. In the second step, MPS is added in order to form the shell of the nanoparticles. Once MPS is involved into the emulsion polymerization reaction, two kinds of reactions are expected to take place in the system: first, polymerization reaction and, second, hydrolysis and condensation reactions.

Polymerization reaction of MPS takes place in the polymer particles which concerns the MPS molecules swelled in the polymer particles and in water which concerns the MPS molecules dissolved into water (Scheme 1). The polymerization rates in the polymer particle and in the aqueous phase depend therefore on the concentration of MPS and radicals in both phases.

The part of MPS molecules contained in the particles is supposed to be protected from water. Contact with water takes place only at the surface of the polymer particles. However, MPS dissolved into water is susceptible to undergo reactions with water. Therefore, MPS molecules contained in the aqueous phase and on the surface of the particles can hydrolyze into silanetriols. The hydrolysis rate depends on the pH value of the suspension media. Then, the silanetriols being metastable can self-condense into oligomers or cyclic molecules. The condensation rate also depends on the pH value of the suspension medium. The products of hydrolysis and condensation (silanetriols or polysiloxane oligomers) can also copolymerize with styrene when they encounter radicals either in the aqueous phase or in the polymer particles. It is important to notice that polysiloxane oligomers can also precipitate forming water insoluble clusters and/or nanoparticles if their molecular weight is high enough. This means that monomer solubility in the different phases has to be related to the hydrolysis and condensation reactions. This allows to calculate correctly monomer partitioning between the different phases (monomer droplets, polymer particles, and aqueous phase) that depends on the solubility of monomers in water and in the polymer particles. Therefore, the partitioning of MPS and the hydrolysis−condensation rates are the two key parameters that control the overall process.

Process Modeling. The rates of polymerization and hydrolysis−condensation depend on the concentrations of monomers in each phase. Therefore, in the first part of this section, monomer partitioning between the different phases is studied using constant partitioning coefficients. Hydrolysis and condensation reactions are therefore supposed not to influence the monomer partitioning. Polysiloxane oligomers formed in the water phase can enter particles to copolymerize with styrene at the same rate as MPS molecules. The applicability and limitations of this assumption under different reaction conditions are discussed in the following part. The model of free radical copolymerization is then presented based on the concentrations in the different phases. Finally, hydrolysis−condensation reactions are modeled.

Scheme 1. Reaction Mechanisms

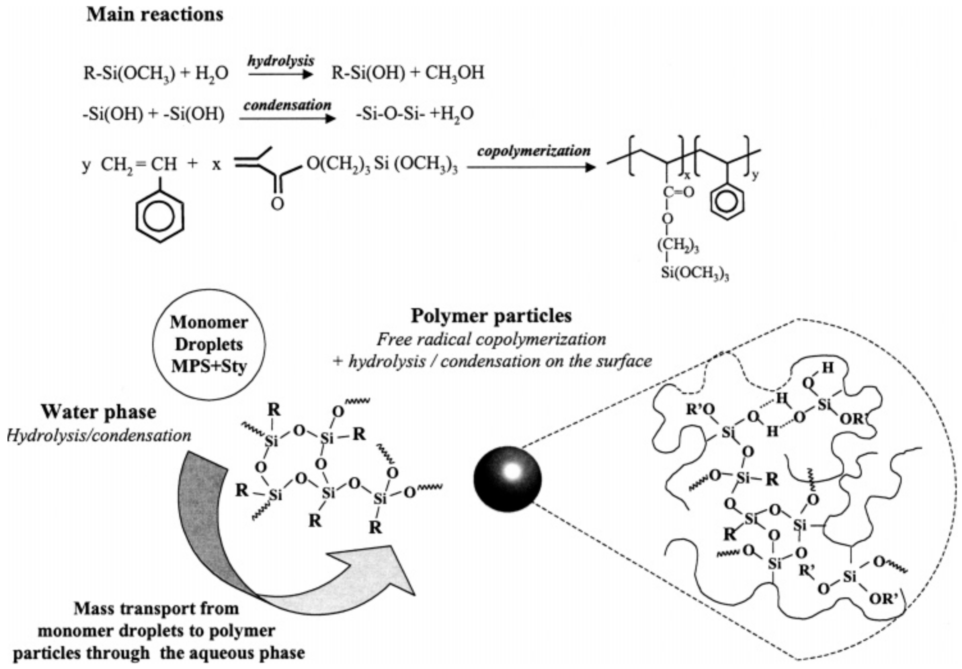

Monomer Partitioning. In emulsion polymerization, the conversion from monomer to polymer occurs principally in the monomer-swollen polymer particles. Monomer is transferred from the monomer droplets to the reaction site by diffusion through the aqueous phase. The polymer particles absorb a certain amount of monomer that is limited by thermodynamic equilibrium. Several models have been developed in the literature to predict the concentration of monomer in the different phases, based on theoretical considerations (thermodynamics, swelling capability of the latex particles by monomer, interactions)[21,22] or on empirical[23,24] or semiempirical relationships.[19,20,25] A review of the three main algorithms used to determine the monomer concentration in the different phases was done by Gugliotta et al.[26] In their work, the authors considered that the model developed by Morton (theoretical model) represents well the monomer partitioning. They reported that constant partition coefficient algorithm was the simplest in terms of number of involved parameters and the time required to solve the corresponding partitioning equations. On the basis of these assumptions, they developed a criterion that helps to choose a model for a specific application. The constant partition coefficient algorithm gives the same results as Morton's model when used to determine the monomer partitioning in seeded and unseeded systems with high solids content, if the monomers are partially soluble in water. Since the monomers used in most of the recipes are usually partially water-soluble, the constant partition coefficient model can be used to calculate the monomer partitioning in the different phases in this case.

In the constant partition coefficient model, the equilibrium distributions among the droplets, particles, and water is described though empirical partition coefficients as follows (where 1 and 2 are styrene and MPS):

$$k_i^j = \frac{\phi_i^j}{\phi_i^{\mathrm{aq}}}, \quad i = 1, 2 \text{ and } j = \mathrm{p, d} \tag{1}$$

and

$$\phi_i^j = \frac{V_i^j}{V^j}, \quad i = 1, 2 \text{ and } j = \mathrm{p, d} \tag{2}$$

where k_i^j is the partition coefficient of monomer i between phase j and the aqueous phase; ϕ_i^j is the volumetric fraction of monomer i in phase j; V_i^j is the volume of monomer i in phase j; V^j is the total volume of phase j; p, d, and aq are the polymer, droplet, and aqueous phases. k_i^j is defined by

Table 3. Coefficients of the Polymerization

coeff	value	ref
r_1	0.45	25
r_2	0.9	25
K_{p11}(cm^3/(mol s)) (STY)	2.9 × 10^6	16
K_{p22}(cm^3/(mol s)) (MPS)	1.44 × 10^6	27

$$k_i^{\mathrm{p}} = \frac{[\mathrm{M}_i^{\mathrm{p}}]}{[\mathrm{M}_i^{\mathrm{aq}}]} = \frac{[\mathrm{M}_i^{\mathrm{p}}]_{\mathrm{sat}}}{[\mathrm{M}_i^{\mathrm{aq}}]_{\mathrm{sat}}}, \quad i = 1, 2$$
$$k_i^{\mathrm{d}} = \frac{\rho_i}{\mathrm{MW}_i[\mathrm{M}_i^{\mathrm{aq}}]_{\mathrm{sat}}}, \quad i = 1, 2 \tag{3}$$

where ρ_i and MW$_i$ are the density and molecular weight of monomer i; $[\mathrm{M}_i^{\mathrm{p}}]_{\mathrm{sat}}$ and $[\mathrm{M}_i^{\mathrm{aq}}]_{\mathrm{sat}}$ are the concentration of saturation of monomer i in the particles and into water. The concentrations of saturation of monomers in the different phases are measured as described in the Experimental Section. The results are shown in Table 1. It should be mentioned that the partitioning coefficients and the partitioning model described above are valid for intervals II and III. In the absence of monomer droplets partitioning takes place between the polymer particles and the aqueous phase.The evolution of the monomer concentrations in the different phases is calculated from the different volumes by solving eqs 1 and 2 from the following relationship:

$$[\mathrm{M}_i^{\mathrm{p}}] = \frac{N_i^{\mathrm{p}}}{V^{\mathrm{p}}} = \frac{V_i^{\mathrm{p}}\rho_i/\mathrm{MW}_i}{V^{\mathrm{p}}}$$
$$[\mathrm{M}_i^{\mathrm{aq}}] = \frac{N_i^{\mathrm{aq}}}{V^{\mathrm{aq}}} = \frac{V_i^{\mathrm{aq}}\rho_i/\mathrm{MW}_i}{V^{\mathrm{aq}}} \tag{4}$$

where

$$V_i^{\mathrm{p}} = \frac{V_i}{1 + \dfrac{k_i^{\mathrm{d}}}{k_i^{\mathrm{p}}}\dfrac{V^{\mathrm{d}}}{V^{\mathrm{p}}} + \dfrac{V^{\mathrm{aq}}}{V^{\mathrm{p}}k_i^{\mathrm{p}}}}, \quad V_i^{\mathrm{d}} = \frac{k_i^{\mathrm{d}}}{k_i^{\mathrm{p}}}\frac{V_i^{\mathrm{p}}}{V^{\mathrm{p}}}V^{\mathrm{d}}, \quad V_i^{\mathrm{aq}} = \frac{V_i^{\mathrm{p}}}{k_i^{\mathrm{p}}}\frac{V^{\mathrm{aq}}}{V^{\mathrm{p}}} \quad \text{interval II} \quad (5)$$

and

$$V_i^{\mathrm{p}} = \frac{V_i}{1 + \dfrac{V^{\mathrm{aq}}}{V^{\mathrm{p}}k_i^{\mathrm{p}}}}, \quad V_i^{\mathrm{aq}} = \frac{V_i^{\mathrm{p}}}{k_i^{\mathrm{p}}}\frac{V^{\mathrm{aq}}}{V^{\mathrm{p}}} \quad \text{interval III} \quad (6)$$

The different volumes are calculated by the following equations assuming that the volume change on mixing is zero and that water does not dissolve in the latex particles:

$$V^{\mathrm{d}} = V_1^{\mathrm{d}} + V_2^{\mathrm{d}}, \quad V^{\mathrm{p}} = V_1^{\mathrm{p}} + V_2^{\mathrm{p}} + V_p^{\mathrm{p}}, \quad V^{\mathrm{aq}} = V_{\mathrm{w}}^{\mathrm{aq}} + V_1^{\mathrm{aq}} + V_2^{\mathrm{aq}} \quad (7)$$

Free Radical Copolymerization Rate. The time variation of the number of moles of each monomer in a perfectly mixed semicontinuous reactor takes the following form:

$$\dot{N}_i = Q_i - R_{\mathrm{p}i}^{\mathrm{p}} - R_{\mathrm{p}i}^{\mathrm{aq}} \quad (8)$$

According to the mechanism of emulsion polymerization, the reaction rate that appears in the material balance is a function of various parameters: monomer concentration in the different phases, $[\mathrm{M}_i^j]$, and number of radicals in each phase (number of moles of radicals in the polymer particles (μ) and number of moles of radicals in the aqueous phase (R_{aq})), as follows:

$$R_{\mathrm{p}i}^{\mathrm{p}} = \mu[\mathrm{M}_i^{\mathrm{p}}](K_{\mathrm{p}1i}P_1^{\mathrm{p}} + K_{\mathrm{p}2i}(1 - P_1^{\mathrm{p}})) \quad (9)$$

and in the aqueous phase

$$R_{\mathrm{p}i}^{\mathrm{aq}} = R_{\mathrm{aq}}[\mathrm{M}_i^{\mathrm{aq}}](K_{\mathrm{p}1i}P_1^{\mathrm{aq}} + K_{\mathrm{p}2i}(1 - P_1^{\mathrm{aq}})) \quad (10)$$

where P_i^j is the time averaged probability that the ultimate unit of an active chain in the phase j be of type i. These probabilities are defined by the following equations:

$$P_i^j = \frac{1}{1 + \dfrac{K_{\mathrm{p}12}[\mathrm{M}_2^j]}{K_{\mathrm{p}21}[\mathrm{M}_1^j]}}, \quad P_2^j = 1 - P_1^j, \quad j = \mathrm{aq, p} \quad (11)$$

The total number of moles radicals in the polymer particles is given by

$$\mu = \frac{\bar{n}N_{\mathrm{p}}V^{\mathrm{aq}}}{N_{\mathrm{A}}} \quad (12)$$

where $\bar{n}$ is the average number of radicals per particle, N_{p} the number of particles per liter, and N_{A} is Avogadro's number. Therefore, $N_{\mathrm{p}}^{\mathrm{T}} = N_{\mathrm{p}}V^{\mathrm{aq}}$. No effort was done to model the concentration of radicals in the polymer particles. μ is estimated from the monomer conversion. The value of $\bar{n}$ was found to be constant after the addition of MPS to the seeded emulsion polymerization where it might undergo interval II or III. The parameters used in the model of partitioning and emulsion copolymerization are listed in Tables 1 and 3.

Hydrolysis Rate. The hydrolysis of the organoalkoxysilane molecule can be written as

$$-\mathrm{Si{-}OCH_3} + \mathrm{H_2O} \xrightarrow{k_{\mathrm{h}}} -\mathrm{Si{-}OH} + \mathrm{CH_3{-}OH} \quad (\mathrm{a})$$

The hydrolysis reaction consumes the methoxysilyl groups (Si−OCH$_3$ that will be noted SiOR) to produce silanol groups (SiOH).

The total number of moles of SiOR groups is the sum of the methoxysilyl groups in the polymer particles, in the aqueous phase, and in the monomer droplets as follows:

$$N_{\mathrm{SiOR}} = N_{\mathrm{SiOR}}^{\mathrm{P}} + N_{\mathrm{SiOR}}^{\mathrm{aq}} + N_{\mathrm{SiOR}}^{\mathrm{d}} \quad (13)$$

The silane molecules in the monomer droplets are supposed not to participate to hydrolysis and condensation reactions since the interaction with water is very small due to the small surface area of the droplets (droplets size = 1×10^{-4} dm). The number of moles of SiOR groups in the droplets is therefore only a function of the monomer partitioning:

$$N_{\mathrm{SiOR}}^{\mathrm{d}} = 3[\mathrm{M}_{\mathrm{MPS}}^{\mathrm{d}}]V^{\mathrm{d}} \quad (14)$$

The hydrolysis of alkoxysilyl groups can take place in the aqueous phase or on the surface of the particles. Inside the particles, alkoxysilyl groups are assumed to be protected from water and can only copolymerize. The concentration of alkoxysilyl groups on the surface of the polymer particles is described as a function of the fraction (f) of the number of alkoxysilyl groups in the particles as follows:

$$[\mathrm{M}_{\mathrm{SiOR}}^{\mathrm{p,surface}}] = f\,[\mathrm{M}_{\mathrm{SiOR}}^{\mathrm{p}}] \quad (0 < f < 1) \quad (15)$$

The parameter f is assumed to be related to the surface area of the particles and to the diffusivity of the SiOR groups in the particles. The hydrolysis rates in the aqueous phase and in the particles can therefore be written as

$$R_{\mathrm{h}}^{\mathrm{aq}} = k_{\mathrm{h}}[\mathrm{M}_{\mathrm{SiOR}}^{\mathrm{aq}}] \quad (16)$$

$$R_{\mathrm{h}}^{\mathrm{p}} = f\,k_{\mathrm{h}}[\mathrm{M}_{\mathrm{SiOR}}^{\mathrm{p}}] \quad (17)$$

$[\mathrm{M}_{\mathrm{SiOR}}^{\mathrm{p}}]$ and $[\mathrm{M}_{\mathrm{SiOR}}^{\mathrm{aq}}]$ are the concentrations of SiOR groups in the particles and in the aqueous phase, respectively.

To study the hydrolysis rate, one can write the material balance of SiOR groups that are consumed by hydrolysis. The mass balance equations of the SiOR in the aqueous phase can be written by considering an input flow rate of SiOR groups coming from droplets, a consumption rate of SiOR groups by hydrolysis and copolymerization, and an output rate of the whole (MPS molecules comprising SiOR and SiOH groups). The main assumption of this model consists of considering that MPS molecules cannot enter particles without passing through water in both batch and semibatch experiments. This gives rise to the following equation:

$$\dot{\mathrm{N}}_{\mathrm{SiOR}}^{\mathrm{aq}} = \mathrm{Q}_{\mathrm{SiOR}}^{\mathrm{in}} - \underbrace{\mathrm{k_h N_{SiOR}^{aq}}}_{\substack{\text{consumed}\\ \text{by hydrolysis}}} - \mathrm{Q}_{\mathrm{MPS}}^{\mathrm{out}} \quad (18)$$

The input flow rate in eq 18 consists of the SiOR groups diffusing to water from the droplets or from the reactor feed if monomer droplets do not exist. The output flow rate is a global output rate of MPS molecules comprising SiOR and SiOH groups. The flow rate of SiOR groups in this total flow rate is the total flow rate times the concentration of SiOR groups in the MPS molecules. The final mass balance equations of the SiOR in the aqueous phase then becomes

$$\dot{\mathrm{N}}_{\mathrm{SiOR}}^{\mathrm{aq}} = \underbrace{3\mathrm{Q}_{\mathrm{MPS}} - 3\dot{\mathrm{N}}_{\mathrm{MPS}}^{\mathrm{d}}}_{\text{input}} - \underbrace{\mathrm{k_h N_{SiOR}^{aq}}}_{\substack{\text{consumed}\\ \text{by hydrolysis}}} - \underbrace{\left(\dot{\mathrm{N}}_{\mathrm{MPS}}^{\mathrm{p}} + \dot{\mathrm{N}}_{\mathrm{PMPS}}^{\mathrm{p}}\right)}_{\substack{\text{output rate}\\ \text{to particles(mon+poly)}}} \underbrace{\frac{\mathrm{N_{SiOR}^{aq}}}{\mathrm{N_{MPS}^{aq}}}}_{\substack{\text{molar ratio}\\ \text{of SiOR groups}}} \quad (19)$$

Let us consider first the "input" term in eq 19. In interval II in a semicontinuous process, the added monomer is stored in the monomer droplets and the concentration of monomer in water does not change. In interval III, the added monomer is supposed to go to the aqueous phase for a sample of time.

Table 4. Optimization Results of *f* and $\bar{n}$

reaction conditions	f	$\bar{n}$
pH = 7, [MPS] = 50 wt % of the shell with Ralufon (D_p = 140 nm)	0.065	0.072
pH = 8.5, [MPS] = 50 wt % of the shell with Ralufon	0.03	0.072
pH = 7, [MPS] = 70 wt % of the shell with Ralufon	0.01	0.05
pH = 7, [MPS] = 50 wt % of the shell with SDS (D_p = 50 nm)	0.0209	

However, the input flow rate of MPS (from water to particles) has to be taken into account in the material balance even under starved conditions. In batch processes, the monomer flow rate equals 0, and therefore any change in the concentration of MPS in the monomer droplets is supposed to generate an increase of MPS into water. The model remains valid.

Let us consider now the output flow rate of SiOR groups. The amount of SiOR groups entering particles is equal to the variation of the number of moles of MPS and PMPS in the polymer particles times the concentration (molar ratio) of SiOR groups in the MPS molecules. N^{p}_{PMPS} is the number of moles of MPS converted to polymer:

$$\dot{N}^{p}_{PMPS} = R^{p}_{pMPS} \tag{20}$$

By the same way, the mass balance equations of the SiOR groups in the polymer particles can be written as

$$\dot{N}^{p}_{SiOR} = -fk_h N^{p}_{SiOR} + \underbrace{\left(\dot{N}^{p}_{MPS} + \dot{N}^{p}_{PMPS}\right)}_{\substack{\text{input}\\ \text{to particles(mon+poly)}}} \frac{N^{aq}_{SiOR}}{N^{aq}_{MPS}} \tag{21}$$

Condensation Rates. The condensation reaction can be written as

$$-\text{Si}-\text{OH} + -\text{Si}-\text{OH} \xrightarrow{k_c} -\text{Si}-\text{O}-\text{Si}- + \text{H}_2\text{O} \tag{b}$$

The silanol groups (SiOH) produced by the hydrolysis reaction of the organoalkoxysilane molecules condense to give rise to siloxane bonds. The condensation rate in the aqueous phase and in the particles is thus proportional to the square of the concentration of SiOH groups in the corresponding phases:

$$R^{aq}_{c} = k_c[\text{M}^{aq}_{SiOH}]^2 \tag{22}$$

$$R^{p}_{c} = k_c'[\text{M}^{p}_{SiOH}]^2 \tag{23}$$

where k_c and k_c' are the condensation rate coefficients in water and in the polymer particles, respectively. As shown in previous works, the condensation rate depends on the nature of the polymer chains.[9] SiOH groups incorporated into polystyrene particles are less prone to condense than when MPS is reacted with butyl acrylate, for instance. This may be due to the rigidity of the polymer chains that reduces the probability of reaction of the silanol groups trapped within the particles. The condensation rate coefficient in the polymer particles is therefore expected to be different from that into water:

$$k_c' = \frac{[\text{M}^{p}_{MPS}]}{[\text{M}^{p}_{PMPS}] + [\text{M}^{p}_{MPS}]} k_c \tag{24}$$

To represent the condensation rate, one can write the material balance of SiOH groups consumed by condensation. The mass balance of SiOH groups in the aqueous phase can therefore be written as

$$\dot{N}^{aq}_{SiOH} = \underbrace{k_h N^{aq}_{SiOR}}_{\substack{\text{produced}\\ \text{by hydrolysis}}} - \underbrace{k_c\left(N^{aq}_{SiOH}\right)^2 / V^{aq}}_{\substack{\text{consumed}\\ \text{by condensation}}} - \underbrace{\left(\dot{N}^{p}_{MPS} + \dot{N}^{p}_{PMPS}\right)}_{\substack{\text{output}\\ \text{to particles (mon+poly)}}} \frac{N^{aq}_{SiOH}}{N^{aq}_{MPS}} \tag{25}$$

Similarly, the mass balance of SiOH groups in the polymer particles writes

$$\dot{N}^{p}_{SiOH} = \underbrace{fk_h N^{p}_{SiOR}}_{\substack{\text{produced}\\ \text{by hydrolysis}}} - \underbrace{k_c'\left(N^{aq}_{SiOH}\right)^2 / V^{aq}}_{\substack{\text{consumed}\\ \text{by condensation}}} + \underbrace{\left(\dot{N}^{p}_{MPS} + \dot{N}^{p}_{PMPS}\right)}_{\substack{\text{output}\\ \text{to particles (mon+poly)}}} \frac{N^{aq}_{SiOH}}{N^{aq}_{MPS}} \tag{26}$$

The total number of moles of SiOH groups is given by

$$N_{SiOH} = N^{p}_{SiOH} + N^{aq}_{SiOH} \tag{27}$$

It can also be obtained from the material balance of hydrolysis as

$$N_{SiOH} = 3N^{T}_{MPS} - N_{SiOR} \tag{28}$$

In the above equations, the concentrations of monomers in the different phases are obtained by the partitioning model (eqs 1−7) and the monomer conversions are obtained from the material balance of monomers (eqs 8−12). The several parts of the model have therefore to be simulated simultaneously in order to obtain the hydrolysis and condensation rates.

Results and Discussion

Validation Procedure. The results discussed in this section correspond to the formation of the core−shell particles. The simulation starts when MPS is introduced to the reactor. The homopolymerization of styrene is not simulated. Moreover, as described in the modeling section, particle nucleation is not modeled. The reaction rate is deduced from the monomer conversion.

In the first step, the off-line measured overall monomer conversion is introduced into the model. On the basis of this measurement, the total number of moles of radicals in the polymer particles (μ) is estimated by optimization by running eqs 1−12 simultaneously. The parameters given in Tables 1−3 were used in the simulation. Since the total number of particles (N^{T}_{p}) is constant during the formation of the shell, $\bar{n}$ can be estimated from μ on the basis of the measured value of N^{T}_{p}. Once $\bar{n}$ is estimated, the concentrations of monomers in the different phases can be calculated using the partitioning model (eqs 1−7) and the material balance of monomers (eqs 8−12). To do that, the partitioning coefficients had to be determined in the absence of reaction. The results of the concentration of monomer in the polymer particles and in water under saturation are presented in Table 1. This allows the calculation of the partitioning coefficients also presented in Table 1. The concentration of radicals in the aqueous phase (R_{aq}) is calculated from an open loop balance of the initiator concentration as a function of the reaction temperature.

These concentrations are then used in order to estimate the hydrolysis (eqs 19, 21) and condensation rates (eqs 25, 26), the hydrolysis and condensation rate coefficients (k_h and k_c) being measured in ethanol−water solution by a series of ^{29}Si liquid-state NMR before the reaction. These results are shown in Table 2. These data allow the identification of the unknown parameters of the model. An optimization method was used to compare the results of the model with the real rates of hydrolysis

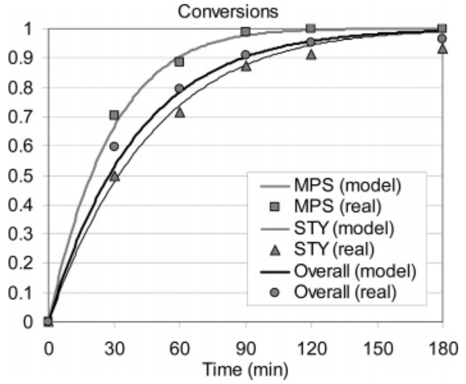

Figure 1. Overall conversion and individual conversions of MPS and STY obtained experimentally and using the model (pH = 7 and [MPS] = 50 wt % of the shell).

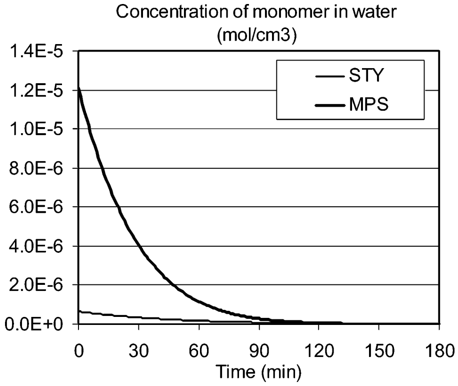

Figure 2. Concentration of monomer in water (pH = 7 and [MPS] = 50 wt % of the shell).

and condensation until convergence. With these parameters, a whole reconstruction of the process can be obtained. The concentrations of monomers and hydrolyzed and condensed groups can be estimated in the different phases.

Estimation of $\bar{n}$. As mentioned above, the first step of the model consists of estimating $\bar{n}$ since it is not modeled in this work. Estimation of $\bar{n}$ is done using the overall and individual monomer conversions. $\bar{n}$ was found to be constant during shell formation.

Figure 1 shows the results of the optimization of $\bar{n}$ for an experiment performed at pH = 7 and [MPS] = 50 wt % of the shell. The overall and individual monomer conversions are allowed to converge to the real values. The conversion of styrene is set to zero when MPS is added in order to represent the conversion evolution in the presence of MPS. The formation of the core is not shown here. Time zero corresponds to the time where MPS is introduced. The values of $\bar{n}$ obtained by optimization of the different experiments of this work are shown in Table 4. It should be mentioned that the values of $\bar{n}$ are dependent on the value of K_{P11} used for styrene. Since several values are proposed in the literature, we chose the more recent reference.[16] The resulting $\bar{n}$ is then used in the model to obtain the reaction rates and the concentrations of monomer in the different phases (Figures 2 and 3). It can be seen that the reaction rate of MPS is higher than that of STY in water due to its higher solubility into water. The reverse is observed in the polymer particles.

By the same way, the polymer composition can be calculated from these data. Figures 4 and 5 show the cumulated polymer mass composition produced in the experiments with pH = 7 and either [MPS] = 50 or 70 wt % of the shell, respectively. The increase of the MPS concentration in the shell affects importantly the polymer composition but also the reaction rate. The optimized value of $\bar{n}$ decreased importantly with increasing the MPS concentration. This joins the ideas mentioned in the literature concerning the limitations in the monomer conversion with increasing the MPS concentration.

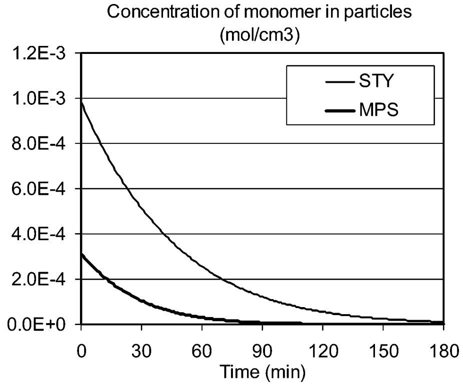

Figure 3. Concentration of monomer in latex particles (pH = 7 and [MPS] = 50 wt % of the shell).

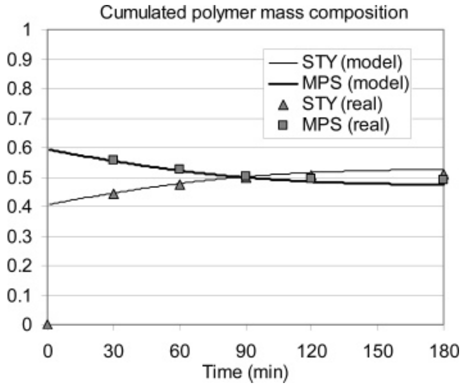

Figure 4. Cumulated polymer mass composition obtained experimentally and using the model (pH = 7 and [MPS] = 50 wt % of the shell).

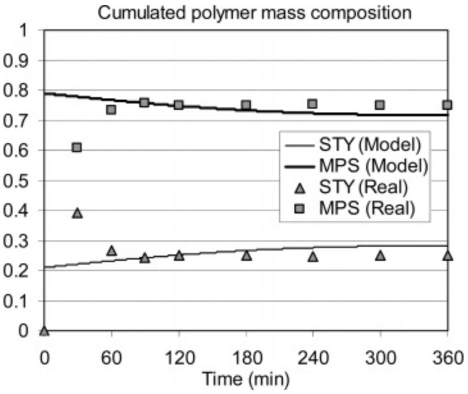

Figure 5. Cumulated polymer mass composition obtained experimentally and using the model (pH = 7 and [MPS] = 70 wt % of the shell).

Estimation of the Hydrolysis Rate. As mentioned above, in the second step of the model, the real data of hydrolysis are used to identify the parameter *f*. Different values of *f* could be obtained from the different reaction conditions (Table 4).

Influence of the pH Value. The pH of the suspension medium is an important parameter in terms of the

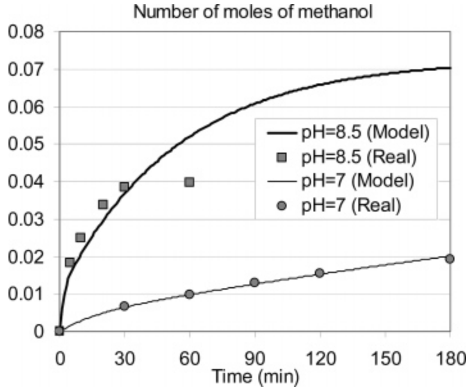

Figure 6. Number of moles of methanol resulting from the hydrolysis reactions at pH = 7 and at pH = 8.5 ([MPS] = 50 wt % of the shell).

process kinetics. It affects the hydrolysis, and therefore the condensation rates and plays an important role concerning the stability and microstructure of the nanoparticles.[9,11]

The hydrolysis rate coefficients were measured in the absence of reaction. The results are given in Table 2 for pH = 7 and pH = 8.5. A higher hydrolysis rate coefficient was obtained in basic conditions than in neutral conditions.

Two experiments were done in order to study the influence of the pH value on the hydrolysis kinetics at pH = 7 and pH = 8.5 with a low amount of MPS (50 wt % MPS of the shell which corresponds to 10 wt % MPS with respect to the total amount of styrene). Lower pH values were avoided since this causes the emulsion system to turn into a gel as a result of the strong interaction of the SiOH groups at the particles surface.[9,11]

Figure 6 shows the methanol concentration obtained with these two experiments. In this figure, the identification of the parameter f is done. The value of f was found to be equal to 0.0654 at pH = 7 and 0.0304 at pH = 8.5 (Table 4). The small value of f indicates that only a small fraction of monomer in the polymer particles participates to hydrolysis. In basic conditions, the parameter f is less than in neutral conditions. This may be due to higher cross-linking of the hybrid copolymer network formed under basic conditions. Indeed, it is known that acid catalysis promotes the formation of weakly cross-linked polymeric structures, while more highly cross-linked, even fully dense inorganic networks are formed in alkaline solutions. This decreases the free volume and increases the viscosity of the swollen particles, which prevents the movement of polymer chains inside the particles. This makes it difficult for SiOR groups to diffuse onto the particle surface although they have a hydrophilic nature.

The figure shows that the concentration of SiOH groups increases importantly with pH which is due to the higher hydrolysis rate coefficient in basic conditions. A higher hydrolysis rate can also be detected at the beginning of the reaction while a high concentration of MPS is in water. Afterward, the concentration of MPS in water decreases since MPS enters the polymer particles and participates in the copolymerization which decreases the hydrolysis rate. In the polymer particles, hydrolysis concerns only the SiOR groups on the surface.

Influence of the Particles Size. To investigate the effect of the particle size, two surfactants, Ralufon and SDS (dodecyl sulfate, sodium salt), were used with the same recipe to produce the hybrid particles. The pH of the medium was 7, and the MPS concentration was 50 mass % in the shell, which corresponds to 10 wt % of the total STY comprising the core. Different particle sizes were obtained with these experiments: 140 and 50 nm, respectively. The diameter of the latex particles (D_p) was measured by dynamic light scattering (DLS) using a Malvern Autosizer Lo-C instrument. Figure 7 shows the number of moles of methanol obtained in each case. A higher hydrolysis rate can be detected with the experiment realized with SDS, for which the particles size is smaller. The decrease in the particles size resulted in an increase of the particles total surface area which, in turn, increased the contact of SiOR groups with the aqueous phase. This was detected by the optimization of the parameter f that was found to be higher (Table 4) than when Ralufon was used as surfactant. As we mentioned in the modeling part, f is proportional to the particles surface area. The given particles size in Table 4 corresponds to that obtained at the end of the formation of the shell.

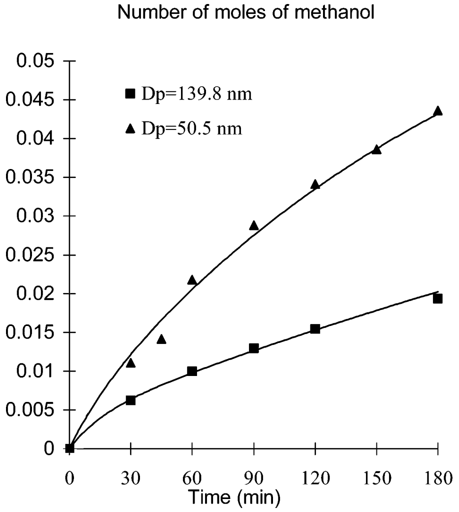

Figure 7. Evolution of the number of moles of methanol with different diameters with SDS (D_p = 50 nm) and Ralufon (D_p = 140 nm) (pH = 7 and [MPS] = 50% weight of the shell).

The increase of the parameter f is supposed to increase the hydrolysis rate in the polymer particles, and therefore the overall concentration of SiOH groups was higher.

Influence of Initial Monomer Composition. The initial monomer composition (ratio of MPS to STY) was varied in order to study its influence on the hydrolysis rate. Two experiments were realized with [MPS] = 50 and 70 wt % of the shell.

The results of these experiments are shown in Figure 8. Changing the concentration of MPS affects the monomer partitioning and therefore the hydrolysis rate as well as the copolymerization rate. Increasing the MPS to STY ratio decreases importantly the reaction rate (see $\bar{n}$ in Table 4).

Moreover, the monomer partitioning is affected. The concentration of MPS in the aqueous phase might increase as shown in Figure 9 for these experiments. If the concentration of MPS in the aqueous phase increases, the hydrolysis rate is supposed to increase, too.

Increasing the MPS to STY ratio might affect the hydrolysis rate by two ways. First, if the concentration of MPS in water is affected, then the hydrolysis rate is affected, too. In the case where the aqueous phase is

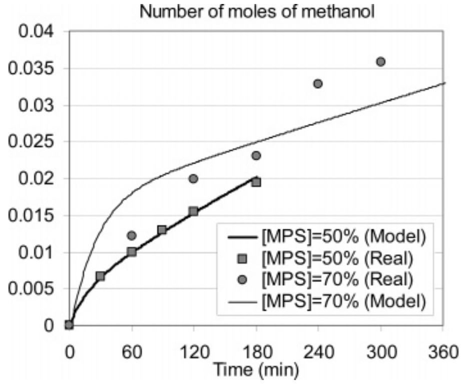

Figure 8. Number of moles of methanol with [MPS] = 50 and 70 wt % of the shell.

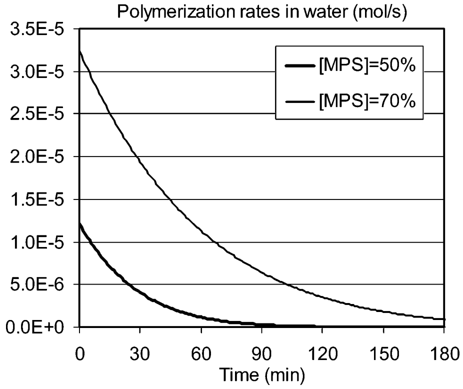

Figure 9. Concentration of MPS in the aqueous phase with [MPS] = 50 and 70 wt % of the shell.

already saturated with MPS, increasing the MPS concentration will not affect the hydrolysis rate in water since the excess of monomer will be stored in the droplets that are protected from hydrolysis. Second, increasing the MPS to STY ratio affects the cross-linking that might affect the hydrolysis on the surface of the particles by decreasing the diffusion of SiOR groups to the surface, which decreases the parameter f.

Estimation of the Condensation Rate. The material balance of SiOH can be calculated on the basis of the identified coefficient of condensation (k_c) and using the concentration of SiOR obtained from the hydrolysis model. No optimization is required in order to predict the concentration of SiOSi groups. The parameter k_c' is calculated using eq 24. Therefore, this part of prediction can be considered as a validation of the model accuracy.

Influence of the pH Value. Since the pH value affects the hydrolysis, it affects also the condensation rate. Increasing the pH value of the suspension medium is supposed to increase the concentration of SiOSi groups in the medium.

Figure 10 shows the evolution of the SiOSi groups in the experiments with different pH values (7 and 8.5) with [MPS] = 50 wt % of the shell. The curve obtained from the model is a complete simulation without any parameter identification by optimization. The figure shows that the concentration of SiOSi groups is more important under basic than under neutral conditions. The model gives a good prediction of the condensation rate. It should be mentioned however that the value of k_c measured at pH = 7 was used in the simulation to predict the condensation rate at pH = 8.5 because the condensation rate was difficult to measure experimentally at pH = 8.5. This might explain the discrepancy between the model predictions and the real data. However, this process can help to identify the k_c parameter at pH = 8.5 as we have done for f.

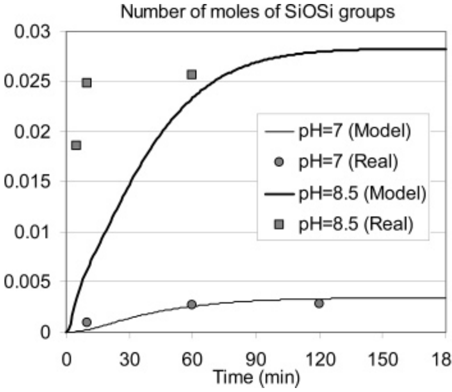

Figure 10. Number of moles of SiOSi groups resulting from the condensation reaction at pH = 7 and pH = 8.5.

Another possibility would be that the monomer partitioning coefficients are dependent on the pH. In the model under hand, these coefficients were assumed to be constant with time and the same for all pH values while it was measured under neutral conditions. However, with high pH values organosilane hydrolyzes into silanetriols drastically. Silanetriol groups become more soluble in water. This affects the silane concentration in the aqueous phase. An expansion of the model would be to write these coefficients as a function of the concentration of the SiOH groups that are affected by both the pH value and the concentration of MPS in the aqueous phase. In these both cases, MPS hydrolyzes and condenses into oligomers rapidly, resulting in the formation of dense clusters which leads to coagulation.

Figure 11 shows the ^{29}Si NMR spectrum of the hybrid nanoparticles at the end of the reaction where pH = 8.5. T^j is the trifunctional alkoxysilane, and j designates the number of siloxane groups bounded to the silicon atom. It is found that most of the silane groups are in the form of T^0 and T^3 in basic conditions. T^0 is the part of silane groups copolymerized into the polymer chain without hydrolysis or condensation. Since in basic conditions the hydrolysis and condensation is very rapid in the aqueous phase, most of the silane groups in the aqueous phase are converted into T^3 before entering the particles. Therefore, T^1 and T^2 do not represent an important ratio in the analyzed hybrid polymer particles.

Influence of Initial Monomer Composition. Since the MPS to STY ratio might affect the hydrolysis rate, it is assumed to affect the condensation rate, too. Figure 12 shows the evolution of the number of moles of SiOSi groups obtained with two experiments with [MPS] = 50 and 70 wt % of the shell. As mentioned above, this figure was obtained from the model without any optimization based on the values of $\bar{n}$ and f found in parts 1 and 2 of the model.

The figure shows that the condensation rate increases with increasing the MPS concentration. This is due to the fact that the hydrolysis rate increases too for the reasons mentioned above: increase of the concentration of MPS in water and decrease of the value of f due to the decrease of the chain mobility in the polymer particles.

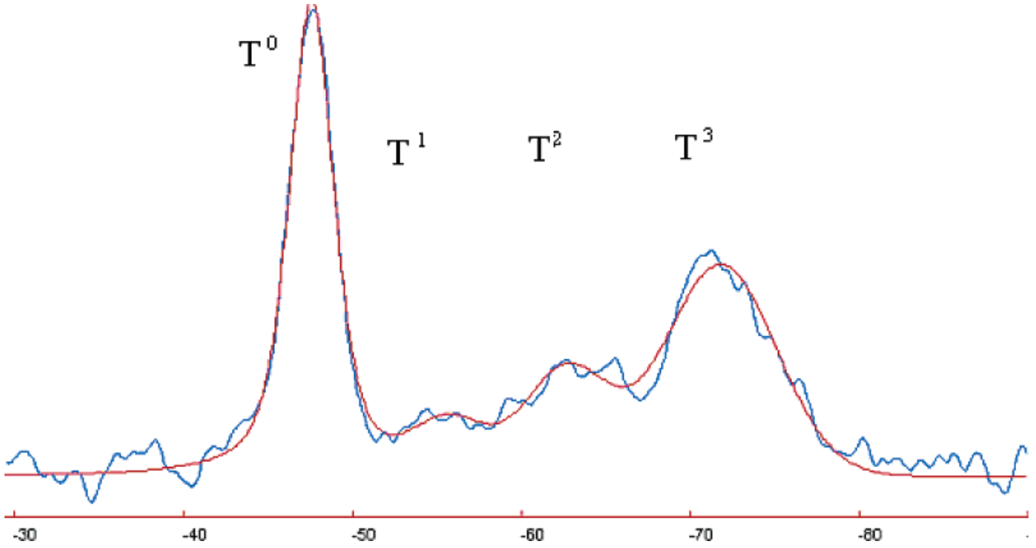

Figure 11. Solid-state ^{29}Si NMR spectrum of the hybrid particles obtained at pH = 8.5.

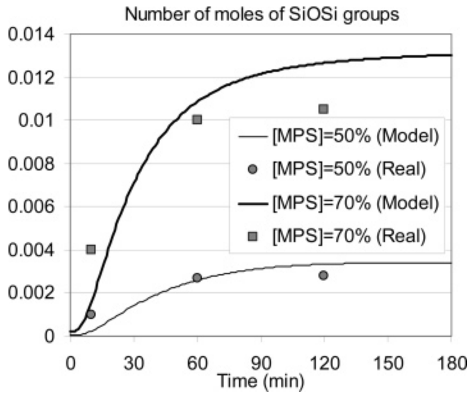

Figure 12. Number of moles of SiOSi groups resulting from the condensation reaction at pH = 7 and [MPS] = 50 and 70 wt % of the shell.

Conclusion

In this work, modeling of the emulsion copolymerization process of styrene with γ-methacryloyloxypropyltrimethoxysilane to yield hybrid core−shell particles is proposed. The organic−inorganic hybrid core−shell nanoparticles were synthesized in a two-step process: emulsion polymerization of styrene and subsequent copolymerization of unreacted styrene with γ-MPS. The modeling takes into account the monomer partitioning between the different phases, the copolymerization rate, the hydrolysis, and condensation rates in the polymer particles and into water.

In the first part of the model, measurement of the unknown process parameters was done. This comprises the concentrations of monomers in the aqueous phase and in the polymer particles and the kinetic parameters such as the hydrolysis rate coefficient and the condensation rate coefficient for different pH values. Next, the process model was used to reconstruct the reaction rates in the different phases and to predict the concentrations of hydrolyzed and condensed groups. The polymer composition was accurately predicted from this model.

The model was tested under different reaction conditions. The pH value of the medium, the particles size, and the MPS to STY ratio were found to affect the hydrolysis and condensation rates. The MPS to STY ratio was found to strongly affect the overall reaction rate and the number of radicals per particles ($\bar{n}$). These phenomena were well represented by the model.

An extension of the model would be to estimate the partitioning coefficients as a function of the reaction parameters (pH, MPS to styrene ratio, etc.) in order to take into account the eventual influence of MPS hydrolysis on monomer partitioning between the different phases.

Nomenclature

Symbols

f	fraction of SiOR groups on the surface of the polymer particles
K_{pji}	propagation rate coefficient of monomer i with radical j (cm^3/(mol s))
k_i^j	partitioning coefficient of monomer i between phase j (d, p) and the aqueous phase
k_h	hydrolysis rate coefficient in the aqueous phase (s^{-1})
k_c	condensation rate coefficient in the aqueous phase (cm^3/(mol s))
k_c'	condensation rate coefficient in the latex particles (cm^3/(mol s))
$[M_i^j]$	concentration of monomer (groups) i in phase j (p, aq, d) (mol/cm^3)
$[M_i^j]_{sat}$	concentration of monomer (groups) i in phase j (p, aq, d) under saturation (mol/cm^3)
$[M]_i^{p,surface}$	concentration of groups i on the surface of the polymer particles (mol/cm^3)
MW_i	molecular weight of monomer i (g/mol)
N_i	residual number of moles of monomer (or groups) i (mol)
N_i^j	residual number of moles of monomer (or groups) i in phase j (p, aq, d) (mol)
N_i^T	total number of moles of monomer i introduced to the reactor (mol)
N_p	number of particle per liter
N_p^T	total number of particle
N_A	Avogadro's number
$\bar{n}$	average number of radicals per particle
P_i^j	probability that the ultimate unit of the chain be of type i in phase j (aq, p)
Q_i	input molar flow rate of monomer i (mol/s)
R_{pi}^j	reaction rate of monomer i in phase j (p, aq) (cm^3)
R_h^j	hydrolysis rate in phase j (aq, p) (mol/(s cm^3))
R_c^j	condensation rate in phase j (aq, p) (mol/(s cm^3))

R_{aq}	number of moles of radicals in the aqueous phase (mol)
V^j	volume of phase j (d = droplets, p = particles, w = water) (cm^3)
V_i^j	volume of monomer i in phase j (d, p, aq) (cm^3)
V_p^p	volume of polymer in the polymer particles (cm^3)
V_w^{aq}	volume of water in the aqueous phase (cm^3)
ρ_i	density of monomer i (g/cm^3)
μ	number of moles of radicals in the polymer particles (mol)
ϕ_i^j	volumetric fraction of monomer i in phase j (d, p, aq)

Notation

MPS	γ-methacryloyloxypropyltrimethoxysilane
PMPS	poly-γ-methacryloyloxypropyltrimethoxysilane
SDS	dodecyl sulfate, sodium salt
SiOR	methoxysilyl group ($Si-OCH_3$)
SiOH	silanol group
STY	styrene

References and Notes

(1) Novak, B. M.; Davies, C. *Macromolecules* **1991**, *24*, 5481−5483.

(2) Tamaki, R.; Naka, K.; Chujo, Y. *Polym. J.* **1998**, *30*, 60.

(3) Wang, Y. T.; Chang, T. C.; Hong, Y. S.; Chen, H. B. *Thermochim. Acta* **2002**, *7145*, 1.

(4) Jang, J.; Park, H. *J. Appl. Polym. Sci.* **2002**, *85*, 2074.

(5) Jackson, C. L.; Bauer, B. J.; Nakatani, A. I.; Barnes, J. D. *Chem. Mater.* **1996**, *8*, 727.

(6) Marcu, I.; Daniels, E. S.; Dimonie, V. L.; Hagiopol, C.; El-Aasser, M. S. *Macromolecules* **2003**, *36*, 326.

(7) Marcu, I.; Daniels, E. S.; Dimonie, V. L.; Roberts, J. E.; El-Aasser, M. S. *Prog. Colloid Polym. Sci.* **2003**, *124*, 31.

(8) Ladika, M.; Rose, G. D. WO95/14700, 2000.

(9) Liles, D. T.; Murray, D. L. US Pat 5932651, 1999.

(10) Roberts, J. E.; Marcu, I.; Dimonie, V.; Daniels, E.; El-Aasser, M. *Polymer Prepr.* **2003**, *44* (1), 277−332.

(11) Bourne, T. R.; Bufkin, B. G.; Wildman, G. C.; Grawe, J. R. *J. Coat. Technol.* **1982**, *54*, 69−82.

(12) Tissot, I.; Novat, C.; Lefebvre, F.; Bourgeat-Lami, E. *Macromolecules* **2001**, *34*, 5737−5739.

(13) Bourgeat-Lami, E.; Tissot, I.; Lefebvre, F. *Macromolecules* **2002**, *35*, 6185−6191.

(14) Tissot, I.; Reymond, J. P.; Lefebvre, F.; Bourgeat-Lami, E. *Chem. Mater.* **2002**, *14*, 1325−1331.

(15) Ni, K. F.; Shan, G. R.; Weng, Z. X.; Sheibat-Othman, N.; Fevotte, G.; Lefebvre, F.; Bourgeat-Lami, E. *Macromolecules* **2005**, *38*, 7321−7329.

(16) Gao, J.; Penlidis, A. *Prog. Polym. Sci.* **2002**, *27*, 403−535.

(17) Sefcik, J.; McCormick, A. V. *Catal. Today* **1997**, *35*, 205−223.

(18) Osterholtz, F. D.; Pohl, E. R. *J. Adhes. Sci.* **1992**, *1*, 127−149.

(19) Maxwell, I. A.; Kurja, J.; Van Doremaele, G. H. J.; German, A. L.; Morrison, B. R. *Makromol. Chem.* **1992**, *193*, 2049−2063.

(20) Noël, L. F. J.; Maxwell, I. A.; German, A. L. *Macromolecules* **1993**, *26*, 2911−2918.

(21) Morton, M.; Kaizermann, S.; Altier, M. W. *J. Colloid Sci.* **1954**, *9*, 300.

(22) Guillot, J. *Makromol. Chem. Suppl.* **1985**, *10/11*, 235.

(23) Armitage, P. D.; De la Cal, J. C.; Asua, J. *J. Appl. Polym. Sci.* **1994**, *51*, 1985−1990.

(24) Omi, S.; Kushibiki, K.; Negishi, M.; Iso, M. *Dep. Chem. Eng., Fac. Technol. Univ. Agric. Technol. Tokyo* **1985**, *184*, 34−49.

(25) Maxwell, I. A.; Kurja, J.; Van Doremaele, G. H. J.; German, A. L.; Morrison, B. R. *Makromol. Chem.* **1992**, *193*, 2065−2080.

(26) Gugliotta, L. M.; Arzamendi, G.; Asua, J. *J. Appl. Polym. Sci.* **1995**, *55*, 1017−1039.

(27) Rao, V. L.; Babu, G. N. *Eur. Polym. J.* **1989**, *6*, 605−609.

MA050999G